

# Luminosity dependence of the cyclotron line and evidence for the accretion regime transition in V 0332+53

Victor Doroshenko<sup>1</sup>, Sergey S. Tsygankov<sup>2,5</sup>, Alexander A. Mushtukov<sup>3,4,5</sup>,  
Alexander A. Lutovinov<sup>5,6</sup>, Andrea Santangelo<sup>1</sup>, Valery F. Suleimanov<sup>1</sup>, Juri Poutanen<sup>2,7</sup>

<sup>1</sup>IAAT, University of Tuebingen, Sand 1, Tuebingen, 72076, Germany

<sup>2</sup>Tuorla Observatory, Department of Physics and Astronomy, University of Turku, Väisäläntie 20, FI-21500 Piikkiö, Finland

<sup>3</sup>Anton Pannekoek Institute, University of Amsterdam, Science Park 904, 1098 XH Amsterdam, The Netherlands

<sup>4</sup>Pulkovo Observatory of the Russian Academy of Sciences, Saint Petersburg 196140, Russia

<sup>5</sup>Space Research Institute of the Russian Academy of Sciences, Profsoyuznaya Str. 84/32, Moscow 117997, Russia

<sup>6</sup>Moscow Institute of Physics and Technology, Moscow region, Dolgoprudnyi, Russia

<sup>7</sup>Nordita, KTH Royal Institute of Technology and Stockholm University, Roslagstullsbacken 23, SE-10691 Stockholm, Sweden

Accepted XXX. Received YYY; in original form ZZZ

## ABSTRACT

We report on the analysis of *NuSTAR* observations of the Be-transient X-ray pulsar V 0332+53 during the giant outburst in 2015 and another minor outburst in 2016. We confirm the cyclotron-line energy – luminosity correlation previously reported in the source and the line energy decrease during the giant outburst. Based on 2016 observations we find that a year later the line energy has increased again essentially reaching the pre-outburst values. We discuss this behaviour and conclude that it is likely caused by a change of the emission region geometry rather than previously suggested accretion-induced decay of the neutron stars magnetic field. At lower luminosities we find for the first time a hint of departure from the anti-correlation of line energy with flux, which we interpret as a transition from super- to sub- critical accretion associated with disappearance of the accretion column. Finally, we confirm and briefly discuss the orbital modulation observed in the outburst light curve of the source.

**Key words:** X-rays: binaries – X-rays: individual: V 0332+53.

## 1 INTRODUCTION

In binary systems accretion of matter supplied by non-degenerate companion onto a strongly magnetised ( $B \sim 10^{12}$  G) rotating neutron star results into pulsed X-ray emission from the vicinity of neutron stars (NSs) magnetic poles. The plasma is channeled to the polar caps by the magnetic field of the neutron star which has also profound effect on the observed X-ray spectra. In particular, the motion of the electrons in strong magnetic field is quantised, which gives rise to the so-called cyclotron resonance scattering features (CRSFs, see Mushtukov et al. (2016) for a recent review). A single (fundamental) or multiple harmonics (Santangelo et al. 1999) absorption-like features can be observed in X-ray band depending on the conditions in the line forming region. In particular, the energy of the fundamental is related to the magnetic field strength as  $E_{\text{cycl}} \sim 12\text{keV } B/10^{12} \text{ G}$ .

The structure of the emission region in the vicinity of the NS and thus the origin of the CRSF are, however, uncertain. At low accretion rates most of the observed emission

likely comes directly from the accretion mounds on the polar caps of the NS where the gravitational energy of the flow is released. However, the observed luminosities of bright pulsars by far exceed the local Eddington limit for kilometre-sized polar caps. At high accretion rates, the plasma must be, therefore, stopped above the NS surface by the radiative pressure and the observed emission has to emerge from the extended “accretion column” (Basko & Sunyaev 1976; Becker et al. 2012; Mushtukov et al. 2015b). Conditions for the transition between the two regimes are determined by the largely unknown geometry of the column, and by the angular- and energy-dependent plasma opacities which makes it extremely hard to make robust theoretical predictions on the transition (critical) luminosity (Mushtukov et al. 2015a,b).

On the other hand, analysis of the luminosity dependence of the observed properties of X-ray pulsars might help to constrain the critical luminosity observationally (Tsygankov et al. 2006; Staubert et al. 2007; Klochkov et al. 2012). Indeed, in low luminous sources the CRSF energy typically increases with the flux, whereas at higher accre-

tion rates an anti-correlation is observed. As discussed by Staubert et al. (2007), Becker et al. (2012), Mushtukov et al. (2015a), and Mushtukov et al. (2015c), this behaviour could point on the two accretion regimes corresponding to sub- and super-critical accretion. Observing the transition between the two regimes in a single source would strongly support this interpretation. In this paper we report on the analysis of the CRSF luminosity dependence in the *Be*-transient X-ray pulsar V 0332+53 during the giant outburst in 2015 and another minor outburst in 2016, and discuss the complex evolution of the line energy throughout the giant outburst and between the two outbursts which, we argue, provides the first evidence for such transition.

## 2 OBSERVATIONS AND DATA ANALYSIS

We focus on the analysis of five dedicated *NuSTAR* observations during the 2015 giant outburst aimed to detect the transition from super- to sub-critical accretion regime. We verify the *NuSTAR* results using the *INTEGRAL*/SPI observations of the source during the outburst (*INTEGRAL* revolutions 1565, 1570, and 1596). Additionally, we report on two follow-up *NuSTAR* observations obtained in Jul 2016 during another periastron passage aimed to extend the observational coverage at low luminosities. We note, that the source flux in the last two observations approaches that for the transition of the source to propeller (Tsygankov et al. 2016), so we probe here the lowest fluxes when the source is still accreting. The observation log is presented in Table 1 and Figs. 1 and 2. Finally, we used also *Swift*/XRT data contemporary to the *NuSTAR* observations to extend the low-energy band and monitor the activity of the source near the periastron passage in July 2016.

The *NuSTAR* data reduction was carried out using the HEASOFT 6.19 package with current calibration files (CALDB version 20160824) and standard data reduction procedures as described in the instruments documentation. Source spectra were extracted from a region of 120'' radius around the V 0332+53. The background spectra were extracted from a circular region of 80'' radius as far away from the source as possible for each observation. The spectra for the two *NuSTAR* units were extracted and fitted simultaneously between 5 and 79 keV for the outburst observations (Fürst et al. 2013), and in 3-79 keV range for the last two observations where no *Swift* data was available. To extract the *Swift*/XRT spectra we used the *Swift* data products service provided by the UK *Swift* Science Data Centre<sup>1</sup> as described in Evans et al. (2009). All *NuSTAR*/*Swift* spectra were grouped to at least 25 counts per bin and fit using the XSPEC version 12.9 with Gehrels weighting (Gehrels 1986).

*INTEGRAL* observed V 0332+53 four times during the spacecraft revolutions 1565, 1570, 1586 and 1596. Problems with the energy calibration of IBIS and JEM-X telescopes did not permit us to reconstruct the source spectrum properly. However, we were able to do it for three observations where the SPI spectrometer was operating (detectors annealing was performed during revolution 1586). The *INTEGRAL*/SPI

data were screened and reduced in accordance with the procedures described by Churazov et al. (2011, 2014).

The broadband spectrum of the source has been previously described (Tsygankov et al. 2006; Lutovinov et al. 2015) using a power law with cutoff at high energies (CUTOFFPL model in XSPEC) modified by interstellar absorption and one to three broad absorption features accounting for the CRSF at  $\sim 26$  keV and its harmonics at  $\sim 50$  keV and  $\sim 72$  keV (Tsygankov et al. 2006). To account for the CRSF and the first harmonic we use the multiplicative gaussian  $G(E) = 1 - D_{\text{cycl}} e^{-\ln 2((E-E_{\text{cycl}})/\sigma_{\text{cycl}})^2}$  rather than exponential gaussian (GABS in Xspec), or the pseudo-lorentzian model (CYCLABS in Xspec) used by Tsygankov et al. (2006). Indeed, the later model was designed to mimic the high energy cutoff (Mihara et al. 1990) which is already included in the continuum model. As a consequence, the measured line centroid  $E_0$  becomes coupled to the cutoff energy and shifted by  $\sigma^2/E_0$  with respect to true centroid (Nakajima et al. 2010), which complicates interpretation of the results. On the other hand, exponential gaussian profile usually used to describe the CRSFs yields a slightly worse fit with systematic  $\sim 1$ -2% residuals around the line, especially for CUTOFFPL continuum. This behaviour has been reported by Pottschmidt et al. (2005) and Nakajima et al. (2010) for 2005 outburst and was interpreted as evidence for a complex CRSF profile. We find, however, that the magnitude of the residuals depends on the continuum model used (for instance, they essentially disappear for HIGHECUT model). Furthermore, restricting the energy range to 20–80 keV as well as using multiplicative gaussian or lorentzian line profile results in no significant residuals for any continuum model. We conclude, therefore, that given the existing uncertainties in modelling of the broadband continuum of X-ray pulsars, there is no strong evidence for a more complex line profile in *NuSTAR* data. This conclusion is consistent with *Swift*/BAT results (Cusumano et al. 2016) where gaussian line provided adequate description of the data.

We verified that measured CRSF centroid does not depend on the continuum or line model used and is well constrained for all *NuSTAR* observations. In particular, we measured consistent CRSF energies (within the uncertainties) using the broadband fits of *NuSTAR*+*Swift*/XRT data and HIGHECUT or a comptonisation model CompTT by Titarchuk (1994), as well as for *NuSTAR* data in 20–80 keV range and the CUTOFFPL model for either lorentzian and gaussian line profiles. In all cases inclusion of the additional soft blackbody component with temperature of  $\sim 0.4$  keV improves the fit for the XRT data, although, taking into account large systematic uncertainties in window-timing mode it is unclear whether this component is real. For all models we also accounted for interstellar absorption. It was sufficient to assume the absorption column fixed to the average value of  $2 \times 10^{22} \text{ cm}^{-2}$  for all observations. We note that the absorption column is similar to one derived from XRT observations in later phases of the outburst (Tsygankov et al. 2016), so there is no evidence for enhanced absorption during the bright phase of the outburst. Neither component significantly affects the derived CRSF parameters. The CompTT continuum model provides, however, the most stable and consistent fit for all observations, therefore, we use this model combined with the gaussian profile for the CRSF for the rest of analysis. On the other hand, *INTEGRAL* data does not allow to reliably constrain the

<sup>1</sup> [http://www.swift.ac.uk/user\\_objects/](http://www.swift.ac.uk/user_objects/)

continuum, so we fix respective parameters to the values derived from the *NuSTAR* data at closest luminosity and only fit for the CRSF parameters. Again, we have verified that the derived line parameters are not significantly affected by choice of the continuum model also in this case. We also found that at low fluxes the width of the first harmonics becomes poorly constrained due to the correlation with continuum temperature. We assumed, therefore, that the relative width of the harmonic (i.e.  $\sigma_{\text{cycl},1}/E_{\text{cycl},1} = \sigma_{\text{cycl}}/E_{\text{cycl}}$ ) is the same at all luminosities. In spectra with highest statistical quality the second harmonic becomes visible in the residuals, although not really significant. This is not surprising as the *NuSTAR* is only sensitive up to 78 keV, so we did not include the second harmonic in the model. The results of the fits are presented in Table. 1. Unfolded spectra for the best-fit model and respective residuals are shown in Fig. 3. All uncertainties are quoted at  $1\sigma$  confidence level and include no systematic error unless stated otherwise.

It is interesting to note that there is an apparent shift by  $\sim 1$  keV between *NuSTAR* and *INTEGRAL* data (which are consistent with each other) and the *Swift*/BAT measurements reported by Cusumano et al. (2016) as illustrated in Fig. 4. This mismatch is probably related to the difference in absolute energy calibration between the instruments as *INTEGRAL* measurements are also consistent for the current and previous outbursts (Ferrigno et al. 2016). Besides this shift, the difference in absolute flux calibration of the instruments and difference in energy ranges used to calculate luminosities needs to be taken into the account for direct comparison of the results. In particular, we re-calculated the *Swift*/BAT luminosities reported by Cusumano et al. (2016) using the *Swift*/BAT 15–50 keV light-curve and contemporary *NuSTAR* fluxes which turn out to be well correlated. Based on this correlation we estimate  $L_x = 91(2)C[10^{37}\text{erg s}^{-1}]$  conversion factor (here  $C$  is observed BAT count-rate). Once said corrections are taken into the account, the CRSF energies measured by all three observatories become compatible within uncertainties as illustrated in Fig. 4.

We also carried out the pulse-phase resolved analysis of all *NuSTAR* observations. The complex spin frequency evolution (Doroshenko et al. 2016) and long intervals between the individual observations prevented us from obtaining a single phase-coherent timing solution. Therefore, we phased all observations using the reference epochs obtained via fitting the CRSF energy pulse profile with a cosine function. The corresponding pulse profiles in 3–15 and 15–80 keV energy bands are also plotted for reference in Fig. 6. For the phase-resolved analysis we additionally fixed the CompTT temperatures and iron line parameters to average values.

### 3 DISCUSSION

#### 3.1 CRSF centroid energy drift

The source is known to exhibit an anti-correlation of the CRSF centroid energy with luminosity which is believed to be caused by change of the accretion column height and was studied extensively during the 2004–2005 outburst (Tsygankov et al. 2006, 2010; Poutanen et al. 2013; Lutovinov et al. 2015). The *NuSTAR*, *INTEGRAL* and *Swift* observations reveal similar behaviour for the current outburst,

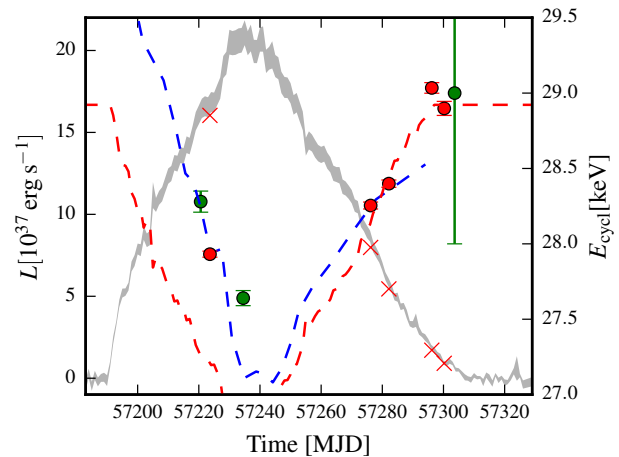


**Figure 1.** *Swift*/BAT light curve in 15–50 keV band (gray) of V 0332+53 during the 2015 giant outburst scaled to match the source luminosity measured using *NuSTAR* pointed observations (red crosses). The red and green circles with error bars indicate the CRSF fundamental energy as measured by *NuSTAR* and *INTEGRAL*/SPI respectively. The red dashed line shows the model prediction for the fundamental energy based on the CRSF energy versus luminosity correlation measured by *NuSTAR* in the declining part of the outburst. The blue dashed line shows the fundamental energy reported by Cusumano et al. (2016) shifted by 1 keV. The shift is likely due to the difference in absolute energy scale of the *Swift*/BAT with respect to *NuSTAR* and SPI.

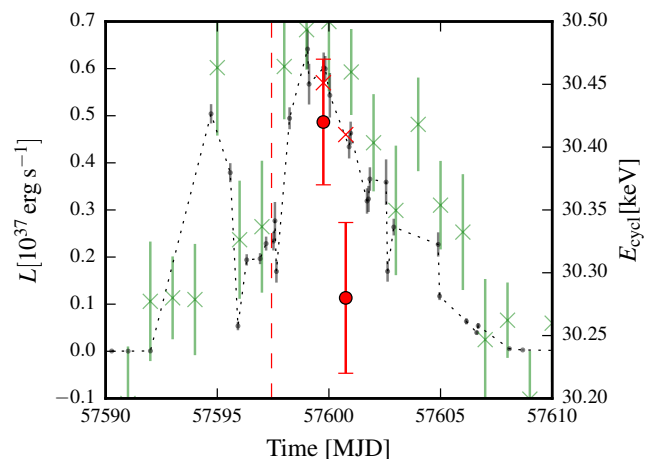


**Figure 2.** *Swift*/XRT (0.3–10 keV, gray points with error bars) and *Swift*/BAT (15–50 keV, green crosses with error bars) light-curves of V 0332+53 during the Aug 2016 periastron passage scaled to match the source luminosity measured using *NuSTAR* pointed observations (red crosses). The red error bars indicate the CRSF fundamental energy as measured by *NuSTAR*.

although with two important differences. First, line energies measured during the declining part of the outburst seem to be significantly lower for comparable luminosity levels (Cusumano et al. 2016) which was not the case in 2005 (Tsygankov et al. 2010). The reported drop of the centroid energy reaches  $\sim 1.5$  keV for *Swift*/BAT data (the blue dashed line in Fig. 1). This is fully consistent with our *NuSTAR* and

**Table 1.** Observation log and best-fit results for the phase averaged spectrum using the **CompTT** model. For INTEGRAL/SPI some of the parameters (shown in *italic*) were fixed to values derived from *NuSTAR* data at closest luminosity level. Luminosity is calculated based on the observed flux in 3–80 keV band not accounting for interstellar absorption or the CRSFs, and assuming distance of 7 kpc.

| Obs. ID.    | Date<br>MJD | Exposure<br>ks | $E_{\text{cycl}}$<br>keV | $\sigma_{\text{cycl}}$<br>keV | $D_{\text{cycl}}$ | $T_0$<br>keV | $kT_e$<br>keV | $\tau$      | $L_{37, 3-80 \text{ keV}}$<br>$10^{37} \text{ erg s}^{-1}$ | $\chi^2/\text{dof}$ |
|-------------|-------------|----------------|--------------------------|-------------------------------|-------------------|--------------|---------------|-------------|--|---------------------|
| 80102002002 | 57223       | 10.5           | 27.93(2)                 | 8.47(8)                       | 0.863(2)          | 1.40(1)      | 5.85(4)       | 16.4(1)     | 16.04  | 0.97/2864           |
| 80102002004 | 57276       | 14.9           | 28.25(2)                 | 7.59(8)                       | 0.861(2)          | 1.19(1)      | 5.73(5)       | 18.3(1)     | 7.98   | 0.9/2628            |
| 80102002006 | 57282       | 17.3           | 28.40(2)                 | 7.43(8)                       | 0.862(2)          | 1.03(2)      | 5.76(5)       | 19.7(1)     | 5.45   | 0.84/2600           |
| 80102002008 | 57296       | 18.2           | 29.03(4)                 | 6.73(8)                       | 0.899(3)          | 0.78(3)      | 6.08(5)       | 18.5(1)     | 1.71   | 0.88/1724           |
| 80102002010 | 57300       | 20.1           | 28.90(5)                 | 6.30(1)                       | 0.895(4)          | 0.73(5)      | 6.09(7)       | 17.7(1)     | 0.91   | 0.83/1375           |
| 90202031002 | 57599.8     | 25.2           | 30.42(5)                 | 6.80(1)                       | 0.925(4)          | 0.66(5)      | 6.80(1)       | 16.5(1)     | 0.57   | 0.88/1369           |
| 90202031004 | 57600.8     | 25.0           | 30.28(6)                 | 6.90(1)                       | 0.921(4)          | 0.68(5)      | 6.90(1)       | 16.4(1)     | 0.46   | 0.91/1330           |
| rev. 1565   | 57220       | 67.8           | 28.28(7)                 | <i>8.47</i>                   | 0.845(5)          | <i>1.4</i>   | <i>5.85</i>   | <i>16.4</i> | $\sim 19.5$  | 0.89/110            |
| rev. 1570   | 57233       | 141.           | 27.64(5)                 | <i>8.47</i>                   | 0.814(4)          | <i>1.4</i>   | <i>5.85</i>   | <i>16.4</i> | $\sim 23.1$  | 1.2/110             |
| rev. 1596   | 57302       | 120.           | 29(2)                    | <i>6.30</i>                   | 0.4(3)            | <i>0.73</i>  | <i>6.1</i>    | <i>17.7</i> | $\sim 1.0$   | 0.88/10             |

*INTEGRAL* results as shown in Figs. 1 and 4. Note that the two *NuSTAR* observations in July 2016 reveal, for the first time, that after the  $\sim 1.5$  keV drop during the 2015 outburst the centroid energy has again increased by same amount effectively negating the observed decay during the outburst.

Cusumano et al. (2016) argued that the observed decrease of the CRSF energy is due to the screening of the NSs dipole magnetic field by the accreting matter. The efficiency of this mechanism depends on the ratio of timescales for field “burial” through the advection by accreting matter and re-emerging of the field driven by magnetic buoyancy, Ohmic diffusion, or other mechanisms (Choudhuri & Konar 2002). While both timescales are highly uncertain, it is still interesting to compare V 0332+53 with other sources where a variation of the CRSF energy with time has been reported. The net decay rate of the CRSF during the outburst is  $\dot{E}_{\text{cycl}} \sim 1.5 \text{ keV}/100 \text{ d}$ , and the net increase rate between the outbursts at least  $\dot{E}_{\text{cycl}} \sim 1.5 \text{ keV}/300 \text{ d}$ . If accretion is indeed responsible for screening of the magnetic field, the field-increase rate shall remain the same also in outburst, so the advection shall reduce the field even faster than observed. The corresponding field decay/re-emerging timescales  $\tau = E_{\text{cycl}}/\dot{E}_{\text{cycl}} \sim 4-16 \text{ yr}$  turn out to be significantly shorter than observed for other sources and generally expected from theoretical point of view. For instance, in Vela X–1 and Her X–1 the CRSF decay rates of  $\sim -9.7 \times 10^{-4} \text{ keV/d}$  (La Parola et al. 2016) and  $\sim -7 \times 10^{-4} \text{ keV/d}$  (Klochkov et al. 2015; Staubert et al. 2016) imply  $\tau \sim 70 - 155 \text{ yr}$ .

Another issue with this interpretation is related to spin evolution of V 0332+53 during the outburst which is governed by balance of the accelerating and braking torques exerted onto the neutron star (Rappaport & Joss 1977, Ghosh & Lamb 1979, Lipunov et al. 1981, Lipunov 1982a, Wang 1987). While both torques increase with the magnetosphere size, the braking torque is more sensitive to the field strength and thus shall decrease faster than the accelerating torque if the intrinsic field of the neutron star indeed drops by  $\sim 5\%$  as suggested by Cusumano et al. (2016). One can, therefore, expect the net spin-up rate of the neutron star to increase during the declining phase of the outburst. However, the opposite is observed as reported by Doroshenko et al. (2016) and illustrated in Fig. 5. The observed spin-up rate actually decreases for a given accretion rate during the later phases of the outburst which implies  $\sim 30\%$  increase of the magnetic

field strength (assuming the torque model by Lipunov (1982b) and  $B = 3.4 \times 10^{12} \text{ G}$  field for the rising phase of the outburst as deduced from the observed CRSF energy, however, similar result can be obtained for Ghosh & Lamb (1979) model). We conclude, therefore, that spin evolution of the source is inconsistent with the intrinsic field decay suggested by Cusumano et al. (2016) and must be related to other factors. Detailed discussion of this issue is out of scope for this work, and we can only speculate that the observed change of the spin-up rate might be associated with viscous evolution of the accretion disc during the outburst. Indeed, the disc is expected to have higher surface density and thus might push further into the magnetosphere during the rising phase of the outburst which would imply lower magnetospheric radius (for the same field strength of the neutron star) and thus higher spin-up rate. We note that comparable total amount of accreted mass during 2005 and 2015 outbursts (Cusumano et al. 2016) together with significantly longer duration of the later outburst suggests that the accretion disc did indeed have different structure in two cases.

So what besides the decay of intrinsic magnetic field could cause the observed CRSF energy decrease? We note that the magnitude of the line energy drop is comparable with the variation of line energy with pulse phase (see Fig. 6) and luminosity, so it is natural to attribute the observed CRSF decay to a change in the geometrical configuration of the line forming region. Such change can be caused by several factors besides the variation of NSs intrinsic field, for instance by a change of the effective magnetospheric radius, which, as discussed above, is also suggested by spin evolution of the pulsar. In context of model by Poutanen et al. (2013), the CRSF is formed via reflection of beamed radiation from the accretion column off the unevenly illuminated NS atmosphere, so the observed change in CRSF energy corresponds to a change of the illumination pattern. The footprint of the accretion column is expected to be reduced for larger magnetospheric radii as the plasma follows the field lines which are closer to the magnetic pole in this case. Decrease of the footprint implies that the accretion column becomes taller for a given luminosity and thus more effectively illuminates equatorial regions of the NS resulting in lower observed CRSF energy as illustrated schematically in Fig. 8.

Changes in the emission region geometry must be reflected in pulse profile shape. Indeed, the pulse profiles ob-

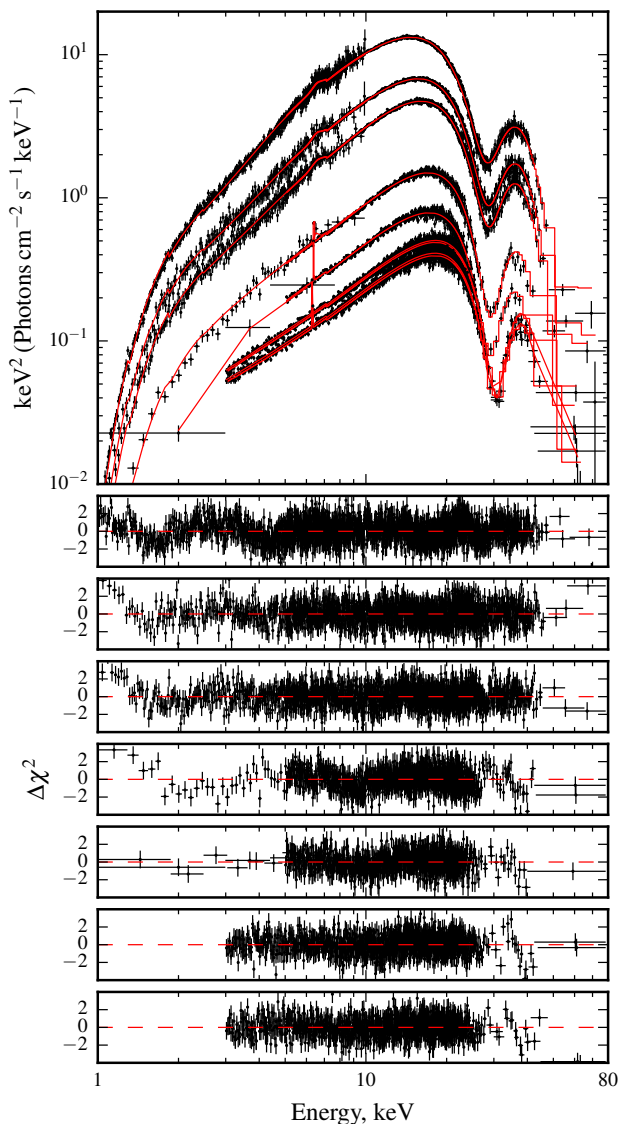


**Figure 3.** Unfolded spectra as observed by *NuSTAR* (5–80 keV) and *Swift*/XRT (1–10 keV), and the corresponding best-fit residuals for the brightest to the dimmest observations (top to bottom, top panel).

served at comparable luminosities in the declining phase of the 2015 outburst and in 2016, do appear to be significantly different as illustrated in Fig. 6. On the other hand, in context of the reflection model almost entire NS surface is illuminated in both cases, so no drastic changes for phase dependence of the CRSF parameters is expected which is again qualitatively consistent with the results of phase resolved analysis. Additional argument supporting the proposed interpretation comes from the comparison of the relative amplitude of the CRSF energy variation with pulse phase in different observations. This turns out to be significantly higher for observations in the declining phase of the outburst where the illuminated area is larger, and thus larger fraction of the NSs atmosphere contributes to the line formation as

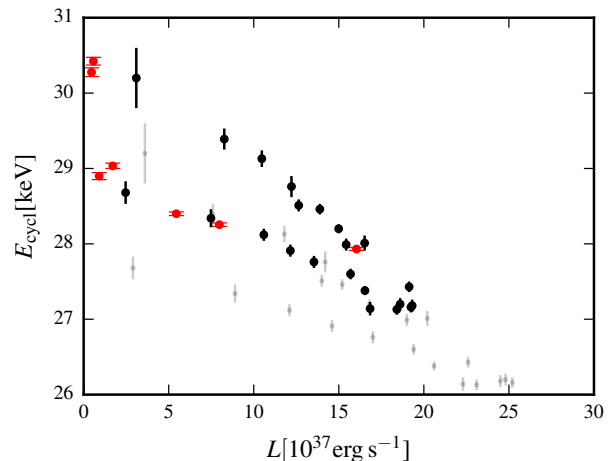


**Figure 4.** Dependence of the fundamental centroid energy on luminosity as observed by *NuSTAR* in 2015–2016 (red points). The same correlation as reported by Cusumano et al. (2016) based on *Swift*/BAT data is also plotted for reference (gray points). Note that the assumed spectral model and energy range used to calculate the luminosity was different in two cases (see text). The apparent  $\sim 1$  keV shift between the two instruments is likely related to difference in their absolute energy calibration. Once this shift and correction to the luminosity are taken into the account, the agreement between *Swift* and other instruments becomes acceptable (black points).

illustrated in Fig. 7. We note that such change indicates a significant change in the emission region structure regardless on assumed model for the CRSF formation.

### 3.2 The critical luminosity

At high luminosities the CRSF centroid energy in V 0332+53 is known to be anti-correlated with flux, which is consistent with Cusumano et al. (2016) findings and our results for the declining phase of the outburst. However, the anti-correlation seems to break at the lowest flux (see Fig. 4). Indeed, the centroid energy is well constrained in the last two *NuSTAR* observations in 2015, and is actually slightly lower during the dimmer observation. Comparison of the observed line energies in two dimmest observations in 2015 implies thus a positive correlation with luminosity with  $dE/dL = 0.16(8)$  keV/ $10^{37}$  erg s $^{-1}$ . For the two observations in 2016, one can deduce  $dE/dL = 1.3(7)$  keV/ $10^{37}$  erg s $^{-1}$ , i.e. in four out of seven *NuSTAR* observations the line energy seems to increase with flux, i.e. the anti-correlation reported for higher fluxes does not seem to extend to low fluxes indefinitely. Transition from an anti-correlation to a correlation is, in fact, expected from theoretical point of view. The anti-correlation observed at high fluxes is thought to be associated with the change of height of the accretion column which is supported by radiative pressure and thus appears only above certain critical luminosity (Basko & Sunyaev 1976). Below the critical flux the line is expected to be correlated with the flux either due to the Doppler effect (Mushtukov et al. 2015c) or due to a change of the atmosphere height above the NS surface driven by ram pressure of the in-falling material (Staubert et al. 2007).

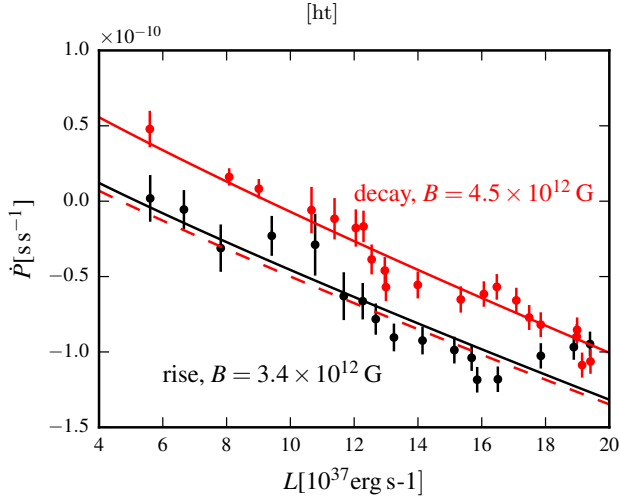


**Figure 5.** Correlation of the spin-up rate with flux as reported in Doroshenko et al. (2016). A best-fit prediction for torque model by Lipunov (1982b) with  $B = 3.4 \times 10^{12}$  G and  $B \sim 4.5 \times 10^{12}$  G for rising (black) and declining (red) parts of the outburst respectively is also shown for reference. A  $\sim 5\%$  magnetic field decay suggested by Cusumano et al. (2016) would imply slightly higher spin-up rate for the declining part of the outburst (with respect to the rising part) as indicated with red dashed line.

Assuming that such a transition does indeed take place, the transitional luminosity can be estimated by fitting a broken linear model to *NuSTAR* and BAT data corrected for the linear drift as shown in Fig. 9. This yields  $L_{\text{crit}} = 0.7^{+0.7}_{-0.1} \times 10^{37}$  erg s $^{-1}$  with  $E_{\text{cycl}} = 30.58(7) - 0.144(4)(L - L_{\text{crit}})/10^{37}$  above the transitional luminosity, and  $E_{\text{cycl}} = 30.58(7) + 1.4(1.2)(L - L_{\text{crit}})/10^{37}$  below it. Here we additionally include in quadrature a systematic uncertainty of 0.1 keV for BAT<sup>2</sup>, and 0.077 keV for *NuSTAR* respectively to get a statistically acceptable fit (in the later case the systematics corresponds to the uncertainty of energy scale around the mean CRSF energy assuming the long-term gain variations reported by Madsen et al. (2015)). The best-fit statistics improves from  $\chi^2_{\text{red}} = 1.37$  for 27 degrees of freedom for a linear fit to  $\chi^2_{\text{red}} = 1.03$  for 25 degrees of freedom for the broken linear fit, which implies that the later model is marginally preferred at  $\sim 3\sigma$  confidence based on the MLR test (Protassov et al. 2002). Note that while the transitional luminosity value seems to be in good agreement with theoretical predictions as illustrated in Fig. 10, both the significance level and the deduced parameters might be affected by the assumptions that the line energy decreased linearly during the giant outburst and has fully recovered between the two outbursts.

On the other hand, the slope of the anti-correlation at high fluxes, which shall be less sensitive to either assumption, is in good agreement with value reported by Tsygankov et al. (2010), i.e. seems to be robustly constrained. We can, therefore, compare it with slopes deduced for the low flux observations as reported above, which implies deviation of  $\sim 3.5\sigma$  and  $\sim 2\sigma$  for 2015 and 2016 observations respectively.

Here we include no systematical uncertainties as the *NuSTAR* gain is expected to remain stable on short timescales. One can also estimate the correlation slope at low luminosities by fitting all four low flux observations with a linear model with a common slope and arbitrary intercepts for 2015 and 2016 low flux observations. This allows to account for the possibility that the line energy has not completely recovered between the outburst as well as for possible long-term energy scale variations. The best-fit  $dE/dL = 0.17(8)$  keV/ $10^{37}$  erg s $^{-1}$  and  $\sim 3.8\sigma$  deviation from the value obtained for higher fluxes.

We conclude, therefore, that *NuSTAR* data provides a first hint of the transition from anti-correlation to correlation of the CRSF energy with flux at low fluxes. As illustrated in Fig. 10, the transitional luminosity is in agreement with theoretical predictions for onset of an accretion column, so it is natural to associate the change in correlation slope with disappearance of the accretion column. On the other hand, comparatively low statistical significance of the correlation break together with the complex evolution of line energy throughout the giant outburst and between the 2015 and 2016 outbursts makes it hard to justify whether the transition is indeed robustly detected, so additional observations are required to confirm our findings.

### 3.3 The “mini”-outburst in 2016

Finally, we would like to comment briefly on the *Swift*/XRT light curve of the source in July–August 2016. Traditionally outbursts of Be-transients are classified in two types, i.e. “giant” ones like that observed from V 0332+53 in 2005, 2015, and “normal” ones which typically occur at periastron and are detectable with all-sky monitors like *Swift*/BAT. Both burst types are evident in long-term V 0332+53 light curve. However, closer inspection reveals also some flux enhancements at almost every periastron with level below that typical for “normal” outbursts. This prompted us to request additional *NuSTAR* observations and *Swift* XRT monitoring which indeed revealed a minor outburst with peak luminosity  $\sim 6 \times 10^{36}$  erg s $^{-1}$  barely detectable also by BAT. We note that even lower-level accretion can occur in V 0332+53 and other Be-transients also when they are not detected by all-sky monitors, and this might have important consequences for studies dedicated to cooling of the neutron stars (Wijnands & Degenaar 2016).

The light curve itself is also quite interesting as it reveals a sharp dip in vicinity of the periastron. Similar behaviour was reported recently by Ferrigno et al. (2016) during the 2015 giant outburst. They interpreted the observed orbital modulation as flux enhancement following the periastron passage associated with the accretion of matter captured at periastron and delayed by propagation through the accretion disc. In our case it is, however, clear, that the outburst starts before the periastron and the accretion rate drops for  $\sim 3$  d to restore later to the pre-dip level (see Fig. 2). We note that light curve modeling by Ferrigno et al. (2016) is not unambiguous and the observed modulation during the giant outburst can be also attributed to the dips at periastron rather than flux enhancement afterwards. We conclude, therefore, that taking into the account our findings, the interpretation or orbital modulation suggested by Ferrigno et al. (2016) is probably not correct. On the other hand, the

<sup>2</sup> <http://heasarc.nasa.gov/docs/heasarc/caldb/swift/docs/bat/SWIFT-BAT-CALDB-ESCALE-v1.pdf>

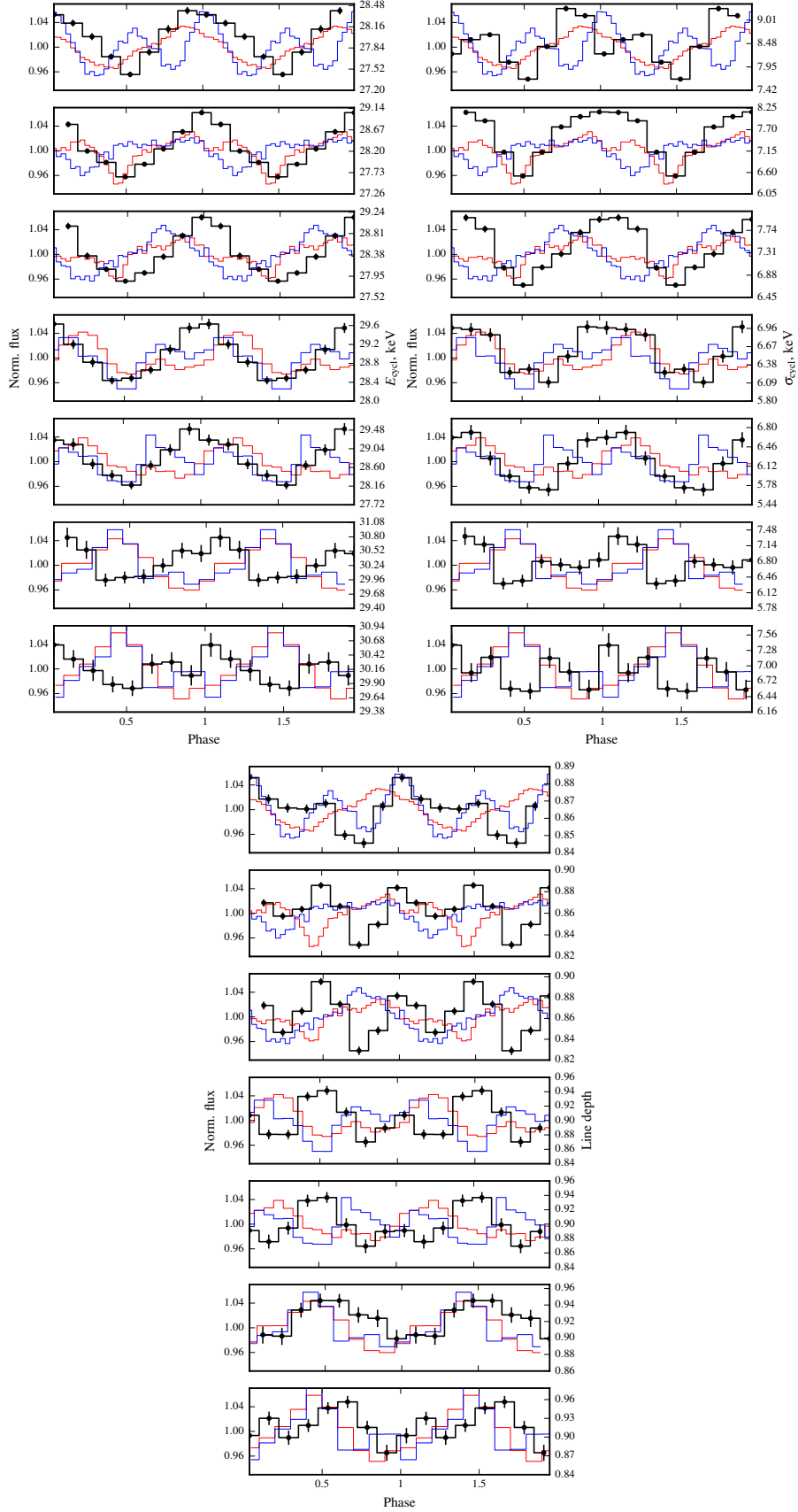


**Figure 6.** Pulse phase dependence of the CRSF energy as observed by *NuSTAR* (black histogram) at different luminosities ( $L/10^{37} \text{ erg s}^{-1} = 16.04, 7.98, 5.45, 1.71, 0.91, 0.57, 0.46$  top to bottom). The pulse profiles in 3–15 and 15–80 keV range (blue and red steps) are also shown. The pulse phase of individual observations was aligned so that zero phase corresponds to maximal CRSF energy.

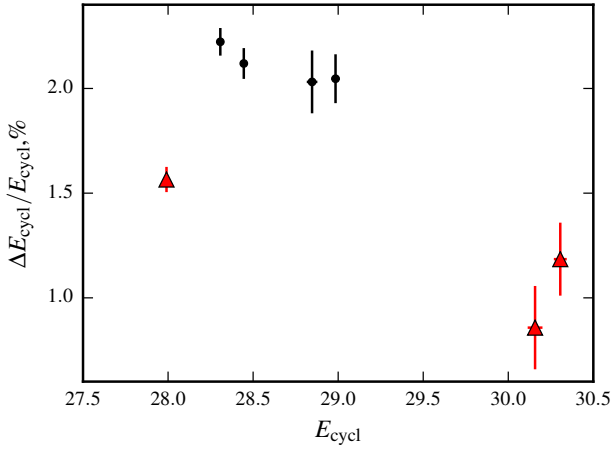


**Figure 7.** Amplitude of variation of the fundamental centroid energy with pulse phase for the declining part of the main outburst (black points) and for the rest of the data (red triangles).

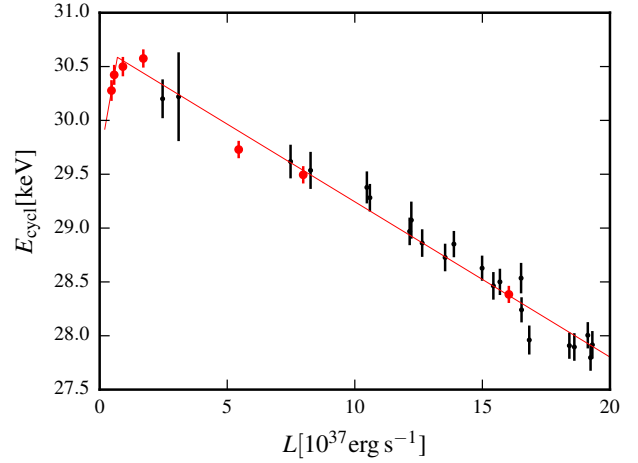


**Figure 9.** Correlation of the CRSF centroid energy on luminosity with the linear drift of  $\dot{E}_{\text{cycl}} = -0.015 \text{ keV/d}$  taken into the account (symbols are the same as in Fig. 4). Note the transition from anti-correlation to correlation below  $10^{37} \text{ erg s}^{-1}$ .

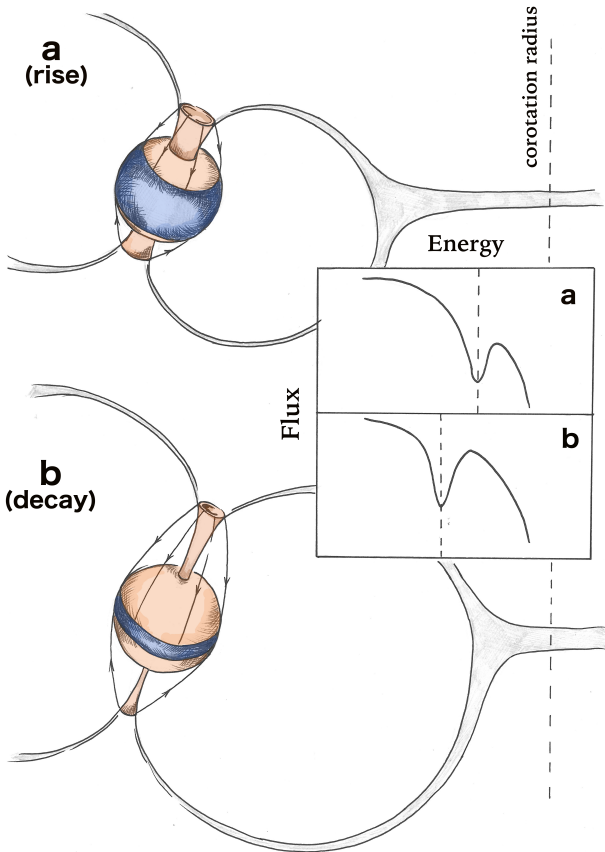


**Figure 8.** Change of the accretion disc structure and of the magnetospheric radius (with respect to the co-rotation radius indicated by vertical line) change both the net torque exerted onto the NS, and the accretion column height. During the declining phase the matter falls closer to the polar areas which increases the height of the accretion column so that illumination pattern shifts to the equatorial areas implying lower observed CRSF energy.

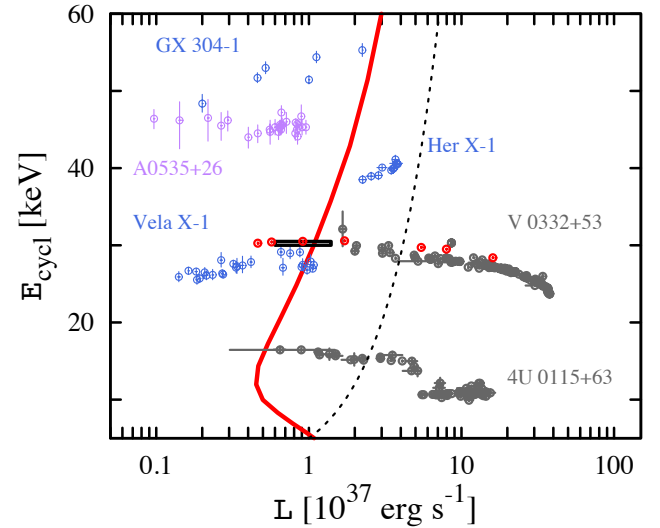


**Figure 10.** CRSF energy as function of luminosity for sources where either a correlation or anti-correlation was reported in the literature. The red circles correspond to *NuSTAR* data reported in this work. The black box corresponds to the estimated value of the transitional luminosity. The red solid curve corresponds to the critical luminosity value (Mushtukov et al. 2015a) for the case of  $\Lambda = 0.5$ , where  $\Lambda$  is the ratio of magnetospheric radius to Alfvén radius, and radiation dominated by X-mode polarisation.

observed flux drop at periastron is at odds with the commonly accepted picture of outbursts in Be-transients which are believed to be triggered by the enhanced accretion as the neutron star passes through the disc of the primary close to the periastron.

Complex outburst development has been reported also for other Be-systems (Postnov et al. 2008; Klochov et al. 2011). For 1A 0535+262 Postnov et al. (2008) attributed the initial flare to unstable accretion triggered by some magnetospheric instability, and the following dip to the depletion

of the inner disc regions. In case of the V 0332+53, however, similar behaviour was observed also during the outburst at high accretion rates, which makes this explanation unlikely. The dip in V 0332+53 is also clearly not related to enhanced absorption as the ratio of XRT/BAT fluxes remains constant. We hesitate to provide a better explanation, and the discussion of physical origin of dips origin is out of scope of this paper. Still, we wanted to bring this issue up to illustrate that exploration of the properties of the Be-transients at low luminosities enabled for the first time by *NuSTAR* and *Swift*/XRT is very interesting indeed and shall be continued.

#### 4 CONCLUSIONS

Based on the analysis of *NuSTAR* observations of V 0332+53 during the declining part of the 2015 giant outburst we have confirmed the previously known anti-correlation of CRSF energy with luminosity. We also confirm the apparent drop of the CRSF centroid energy during the declining part recently interpreted by Cusumano et al. (2016) as the result of the accretion-induced decay of the magnetic field of the NS. We find that line energy decrease is consistent with being time linear throughout the outburst with rate of  $\sim 0.015$  keV/d. Furthermore, follow-up *NuSTAR* observations of another outburst in 2016 revealed that the line energy has increased again approximately to values observed before the 2015 outburst which implies a recovery rate of  $\sim 0.05$  keV/d. Both timescales imply unprecedentedly fast evolution of the magnetic field of the neutron star if the change of the observed line energy is directly related to field strength as suggested by Cusumano et al. (2016). We argue, however, that evolution of the observed CRSF energy is likely instead associated with a change of the emission region geometry. The later is defined by the magnetosphere size which indeed seems to be different in rising and declining parts of the outburst as suggested by the observed spin evolution of the neutron star.

Finally, we find that at luminosities below  $\sim 10^{37}$  erg s $^{-1}$  the anti-correlation of the CRSF energy with flux reported for higher luminosities seems to break, which we interpret as the first observational evidence for the transition from super- to sub-critical accretion. The transitional luminosity is in agreement with the theoretical predictions and cyclotron line luminosity dependence observed in other sources as shown in Fig. 10. We note, however, that taking into the account complex evolution of line energy throughout the outburst and comparatively low statistical significance of the break, the transition can not be considered to be robustly detected and additional observations are required to confirm our findings.

#### ACKNOWLEDGEMENTS

Authors thank E.M. Churazov who developed the INTEGRAL/SPI data analysis methods and provided the software. This research has made use of data provided by HEASARC (NASA/GSFC and Smithsonian Astrophysical Observatory). This work is based on observations with INTEGRAL, an ESA project with instruments and science data centre funded by ESA member states (especially the PI countries: Denmark, France, Germany, Italy, Switzerland, Spain), and with the participation of Russia and the USA. This work made use of data supplied by the UK Swift Science Data Centre at the University of Leicester. The

authors acknowledge support from Deutsches Zentrum für Luft- und Raumfahrt (DLR) through DLR-PT grant 50 OR 0702 (VD), Deutsche Forschungsgemeinschaft (DFG) through WE 1312/48-1 (VS), the Russian Science Foundation through grant 14-12-01287 (AAM, SST, AAL), the Academy of Finland through grant 268740 and the Foundations' Professor Pool, the Finnish Cultural Foundation (JP).

#### REFERENCES

- Basko M. M., Sunyaev R. A., 1976, *MNRAS*, **175**, 395  
 Becker P. A., et al., 2012, *A&A*, **544**, A123  
 Choudhuri A. R., Konar S., 2002, *MNRAS*, **332**, 933  
 Churazov E., et al., 2011, *MNRAS*, **411**, 1727  
 Churazov E., et al., 2014, *Nature*, **512**, 406  
 Cusumano G., La Parola V., D'Ài A., Segreto A., Tagliaferri G., Barthelmy S. D., Gehrels N., 2016, *MNRAS*, **460**, L99  
 Doroshenko V., Tsygankov S., Santangelo A., 2016, *A&A*, **589**, A72  
 Evans P. A., et al., 2009, *MNRAS*, **397**, 1177  
 Ferrigno C., et al., 2016, preprint, ([arXiv:1607.03293](https://arxiv.org/abs/1607.03293))  
 Fürst F., et al., 2013, *ApJ*, **779**, 69  
 Gehrels N., 1986, *ApJ*, **303**, 336  
 Ghosh P., Lamb F. K., 1979, *ApJ*, **234**, 296  
 Klochkov D., Ferrigno C., Santangelo A., Staubert R., Kretschmar P., Caballero I., Postnov K., Wilson-Hodge C. A., 2011, *A&A*, **536**, L8  
 Klochkov D., et al., 2012, *A&A*, **542**, L28  
 Klochkov D., Staubert R., Postnov K., Wilms J., Rothschild R. E., Santangelo A., 2015, *A&A*, **578**, A88  
 La Parola V., Cusumano G., Segreto A., D'Ài A., 2016, *MNRAS*, **463**, 185  
 Lipunov V. M., 1982a, *Ap&SS*, **82**, 343  
 Lipunov V. M., 1982b, *Ap&SS*, **85**, 451  
 Lipunov V. M., Semenov E. S., Shakura N. I., 1981, *Soviet Ast.*, **25**, 439  
 Lutovinov A. A., et al., 2015, *MNRAS*, **448**, 2175  
 Madsen K. K., et al., 2015, *ApJ*, **801**, 66  
 Mihara T., et al., 1990, *Nature*, **346**, 250  
 Mushtukov A. A., et al., 2015a, *MNRAS*, **447**, 1847  
 Mushtukov A. A., et al., 2015b, *MNRAS*, **454**, 2539  
 Mushtukov A. A., et al., 2015c, *MNRAS*, **454**, 2714  
 Mushtukov A. A., Nagirner D. I., Poutanen J., 2016, *Phys. Rev. D*, **93**, 105003  
 Nakajima M., Mihara T., Makishima K., 2010, *ApJ*, **710**, 1755  
 Postnov K., Staubert R., Santangelo A., Klochkov D., Kretschmar P., Caballero I., 2008, *A&A*, **480**, L21  
 Pottschmidt K., et al., 2005, *ApJ*, **634**, L97  
 Poutanen J., et al., 2013, *ApJ*, **777**, 115  
 Protassov R., van Dyk D. A., Connors A., Kashyap V. L., Siemiginowska A., 2002, *ApJ*, **571**, 545  
 Rappaport S., Joss P. C., 1977, *Nature*, **266**, 683  
 Santangelo A., et al., 1999, *ApJ*, **523**, L85  
 Staubert R., et al., 2007, *A&A*, **465**, L25  
 Staubert R., Klochkov D., Vybornov V., Wilms J., Harrison F. A., 2016, *A&A*, **590**, A91  
 Titarchuk L., 1994, *ApJ*, **434**, 570  
 Tsygankov S. S., et al., 2006, *MNRAS*, **371**, 19  
 Tsygankov S. S., Lutovinov A. A., Serber A. V., 2010, *MNRAS*, **401**, 1628  
 Tsygankov S. S., Lutovinov A. A., Doroshenko V., Mushtukov A. A., Suleimanov V., Poutanen J., 2016, *A&A*, **593**, A16  
 Wang Y.-M., 1987, *A&A*, **183**, 257  
 Wijnands R., Degenaar N., 2016, *MNRAS*, **463**, L46

This paper has been typeset from a  $\text{\TeX/L\AA\TeX}$  file prepared by the author.